Expression and Targeting of Human Fibroblast Activation Protein in a Human Skin/Severe Combined Immunodeficient Mouse Breast Cancer Xenograft Model

Kiki Tahtis, Fook-Thean Lee, Jennifer M. Wheatley, Pilar Garin-Chesa, John E. Park, Fiona E. Smyth, Yuichi Obata, Elisabeth Stockert, Cathrine M. Hall, Lloyd J. Old, Wolfgang J. Rettig, and Andrew M. Scott[1]

Tumour Targeting Program, Ludwig Institute for Cancer Research, Melbourne Branch, Austin and Repatriation Medical Centre, Victoria 3084, Australia [K. T., F-T. L., J. M. W., F. E. S., C. M. H., A. M. S.]; Department of Surgery, Austin and Repatriation Medical Centre, Victoria 3084, Australia [J. M. W.]; RIKEN Bioresource Centre, Tsukuba Institute, Tsubuka 305-0074, Japan [Y. O.]; Ludwig Institute for Cancer Research, New York Branch, Memorial Sloan Kettering Cancer Center, New York, New York 10021 [E. S., L. J. O.]; and Department of Oncology Research, Boehringer Ingelheim Pharma KG, 88397 Biberach, Germany [P. G-C., J. E. P., W. J. R.]

Abstract

Antigens and receptors that are highly expressed on tumor stromal cells, such as fibroblast activation protein (FAP), are attractive targets for antibody-based therapies because the supporting stroma and vessel network is essential for a solid neoplasm to grow beyond a size of 1–2 mm. The *in vivo* characterization of antibodies targeting human stromal or vessel antigens is hindered by the lack of an appropriate mouse model system because xenografts in standard mouse models express stromal and vessels elements of murine origin. This limitation may be overcome by the development of a human skin/mouse chimeric model, which is established by transplanting human foreskin on to the lateral flank of severe combined immunodeficient mice. The subsequent inoculation of breast carcinoma MCF-7 cells within the dermis of the transplanted human skin resulted in the production of xenografts expressing stromal and vessel elements of human origin. Widespread expression of human FAP-positive reactive stromal fibroblasts within xenografts was seen up to 2 months posttransplantation and postinjection of cells. Human blood vessel antigen expression also persisted at 2 months posttransplantation and postinjection of cells with murine vessels coexisting with the human vascular supply. The model was subsequently used to evaluate the biodistribution properties of an iodine-131-labeled humanized anti-FAP monoclonal antibody (BIBH-7). The results showed high specific targeting of the stromal compartment of the xenograft, indicating that the model provides a useful and novel approach for the *in vivo* assessment of the immunotherapeutic potential of molecules targeting human stroma and angiogenic systems.

Introduction

Solid neoplasms, including epithelial cancers, require the formation of a supporting stroma if they are to grow beyond the size of 1–2 mm (1). Epithelial cancers induce the formation of stroma, which is a complex extracellular matrix-rich tissue that is primarily comprised of newly formed blood vessels and connective tissue cells such as activated fibroblasts as well as inflammatory infiltrates and a complex network of matrix proteins. The stromal compartment often comprises between 20% and 50% of the mass of a solid tumor. However, depending on the type of neoplasm, the amount and composition of the stroma may vary, and in some histological types of cancer, the stromal compartment may contribute to >90% of the mass of the tumor (1).

Reactive stromal fibroblasts found in injured/healing tissue and epithelial tumors characteristically induce the formation of FAP,[2] a type II integral membrane protein that belongs to the serine protease gene family (2–5). Recent studies have demonstrated that FAP has dipeptidyl peptidase activity, preferentially cleaving NH_2-terminal Ala-Pro dipeptides, and also has gelatinolytic and collagenase activity (3, 5). Detailed immunohistochemical analyses have shown that FAP displays very restricted normal tissue distribution, with resting fibrocytes in normal tissue generally lacking detectable FAP expression (2, 6). Among the nonneoplastic adult lesional tissues examined, expression of FAP has been observed in the activated fibroblasts of healing wounds and in activated hepatic stellate cells during cirrhosis (7), whereas in normal adult tissue only pancreatic islet (A) cells are FAP positive (2, 6). Conversely, FAP-positive stromal fibroblasts are seen in the stroma of over 90% of malignant breast, ovarian, colorectal, lung, skin and pancreatic tumors. A proportion of bone and soft tissue sarcoma tumor cells are also FAP positive (6). Some reports have shown that FAP expression

Received 12/4/02; revised 4/21/03; accepted 5/27/03.
The costs of publication of this article were defrayed in part by the payment of page charges. This article must therefore be hereby marked *advertisement* in accordance with 18 U.S.C. Section 1734 solely to indicate this fact.

[1] To whom requests for reprints should be addressed, at Ludwig Institute for Cancer Research, Austin and Repatriation Medical Centre, Heidelberg, Victoria 3084, Australia. Phone: 613-9496-5876; Fax: 613-9496-5892; E-mail: ams@austin.unimelb.edu.au.

[2] The abbreviations used are: FAP, fibroblast activation protein; Le^y, Lewis y; PECAM-1, platelet endothelial cell adhesion molecule-1; SCID, severe combined immunodeficient; % ID/g, percent injected dose per gram; mAb, monoclonal antibody; p.i., postinjection.

may be an independent prognostic factor in certain tumors such as breast cancer (8).

The targeting of antigens selectively expressed on tumor stroma or tumor capillary endothelial cells with mAbs has emerged as a novel targeting approach for immunotherapy (9–11). The FAP antigen is an attractive antigenic target because it has broad applicability to several common and as yet poorly treatable cancer types, and it also displays a restricted expression pattern in normal tissue (2). However until recently, no relevant tumor model existed that could confirm that antibodies against these tumor compartments could selectively accumulate in human tumor tissues, because xenografts grown in standard mouse models express stromal and vessel elements of murine origin. In this report, the development and characterization of stromal human FAP expression in a human skin/SCID mouse chimeric model are presented. Transplanted skin samples and breast carcinoma xenografts established in the dermis of the grafted skin were characterized for the expression of human HLA-A,B,C, mouse H-2, stromal markers (human FAP), vessel markers (human endoGlyx-1, human PECAM-1, and mouse PECAM-1), and tumor antigens (Le^y). The ability of a ^{131}I-labeled humanized anti-FAP mAb (BIBH-7) to target human FAP-expressing tumor xenografts established in this model was also evaluated, to determine whether specific binding to the stromal components of the tumor could be demonstrated.

Materials and Methods

Antibodies and Cell Lines. MCF-7, a Le^y-expressing estrogen-dependent human breast adenocarcinoma cell line (12) was obtained from American Type Culture Collection (Manassas, VA). MCF-7 cells were cultured in RPMI 1640 supplemented with 10% FCS (CSL Biosciences, Melbourne, Australia) and 50 units/ml penicillin-streptomycin (Life Technologies, Inc., Grand Island, NY). Antibodies were obtained from the following sources. m3S193 and hu3S193 (antihuman Le^y) and control isotype-matched mA33 and huA33 (antihuman A33) antibodies were provided by the Biological Production Facility (Ludwig Institute, Melbourne, Australia). Murine F19 (mF19, mouse antihuman FAPα mAb) and endoGlyx-1 (antihuman endoGlyx-1) were obtained from the New York branch of the Ludwig Institute. Humanized antihuman FAPα antibody (BIBH-7) was obtained from Boehringer Ingelheim (Biberach, Germany). Antihuman PECAM-1 (clone JC/70A), antihuman HLA-A,B,C (clone W6/32), and biotinylated rabbit antirat immunoglobulin were purchased from DAKO Corp. (Carpinteria, CA). Antimouse PECAM-1 (clone MEC13.3) was obtained from PharMingen (San Diego, CA). Rat antimouse H-2 antibody (HD464) was obtained from Dr. Yuichi Obata (Nagoya, Japan). Biotinylated sheep antimouse secondary antibody (γ and light chain specific) and sheep antimouse IgG/IgM (naked and horseradish peroxidase conjugated) antibodies were purchased from Silenus (Melbourne, Australia).

Grafting Procedure and Xenograft Establishment. All animal studies were conducted with approval of the Austin and Repatriation Medical Centre animal ethics committee. Female SCID mice were obtained from the Walter and Elisa Hall Institute and Austin Research Institute animal facilities (Melbourne, Australia) and maintained in autoclaved microisolator cages. The skin transplantation protocol was designed with modifications from previously published studies (13–15). All procedures were performed in a Class 1 laminar flow cabinet. At 6 weeks of age, an ELISA was performed to verify that the serum immunoglobulin levels (IgG and IgM) of SCID mice were less than 50 μg/ml, and only fully immunodeficient mice were used (16). Mice aged 6–8 weeks were anesthetized by i.m. injection of 150 mg/kg ketamine and 5 mg/kg Ilium Xylazil-20 (125 μl/animal; Troy Laboratories, New South Wales, Australia). The graft site was prepared by shaving the hair from a 4-cm^2 area of the lateral dorsum and swabbing with 10% (w/v) povidone-iodine antiseptic solution (Orion Laboratories, Welshpool, Australia). To engraft skin, a circular graft bed of approximately 1.5 cm^2 was prepared by removing skin down to the fascia. Full thickness human foreskin, obtained from elective circumcisions and maintained in sterile saline, was cut to an identical size and placed on the wound bed. All skin grafting was performed within 3 h of patient surgery. The acquisition of human skin tissue was approved by the Human Research Ethics Committee of the Austin and Repatriation Medical Centre (Melbourne, Australia). The wound site was initially covered with a 3-cm^2 piece of sterile jelonet paraffin gauze dressing (Smith and Nephew, Hull, United Kingdom) and then secured with Mefix bandaging (SCA Mölnlycke Clinical Products, Mölnlycke, Sweden) and 13-mm Albupore acrylic adhesive (Smith and Nephew), which were wrapped around the body of the animal, between the limbs. Once the skin grafts were fully healed (approximately 4–6 weeks later), MCF-7 tumor xenografts were established by the injection of 2×10^6 cells in 50 μl of media intradermally into the transplants, using a 29-gauge 0.5-ml insulin syringe (Terumo Medical Corp., Elkton, MD). A slow-release estrogen pellet (0.72 mg of 17β-estradiol; Innovative Research of America, Sarasota, FL) was implanted s.c. in the scapular region at the same time as injection of tumor cells, using a small incision closed by a single stitch using silk 5/0 nonabsorbable sutures (B. Braun Surgical, Melsungen, Germany). Control SCID mice also received estradiol pellet implants and 2×10^6 MCF-7 cells in the lateral flank for establishment of MCF-7 xenografts under murine skin. The establishment of tumors and tumor growth rate were monitored by tumor volume measurement [(length $\times$ width^2)/2] every 2–3 days, where length was the longest axis, and width was the measurement at right angles to length (17).

Immunohistochemical Characterization of Transplanted Skin and Xenografts. At 1, 2, 3, 4, 6, 8, 10, and 12 weeks posttransplantation, mice were sacrificed, and human transplanted skin with adjacent mouse skin was harvested for analysis. MCF-7 xenografts grown within grafted ($n = 33$) and control ($n = 15$) SCID mice were harvested at 2, 3, 4, 5, 6, 7, and 9 weeks p.i. of tumor cells. Excised samples were snap frozen in liquid nitrogen and then stored at -80°C for immunohistochemical analysis. Sequential 5-μm sections were cut from frozen specimens on the day of staining. Slides were fixed in cold acetone (4°C for 10 min), air dried, rehydrated in PBS, and then blocked with 10% FCS in PBS for 20 min at room temperature. Slides were blotted, primary antibody was applied at optimal concentration (determined

from prior titration), and slides were incubated for 30 min at room temperature. Slides were subsequently washed, and secondary antibodies (biotinylated sheep antimouse or biotinylated rabbit antirat at 1:400 and 1:500 dilutions, respectively) were applied. After washing in PBS, the antibody conjugate was visualized using the Vectastain ABC Elite Kit (Vector Laboratories, Burlingame, CA) with 3-amino-9-ethylcarbazole as the chromagen (Sigma Chemical Co., St. Louis, MO). All slides were counterstained for 5–7 min with Meyers hematoxylin. Double staining immunohistochemistry was performed using the DAKO EnVision+ System (DAKO Corp.) according to the manufacturer's instructions.

Radiolabeling and Biodistribution. Radioiodination of BIBH-7 with ^{131}I and ^{125}I (New England Nuclear Life Science Products, Boston, MA) was performed via a modified chloramine-T (Merck, Darmstadt, Germany) reaction, using a chloramine-T:protein ratio of 4:1 (18). The immunoreactivity, affinity, and serum stability at 37°C for radiolabeled BIBH-7 were determined as described previously (17). The biodistribution analysis involved 19 grafted mice that were divided into two groups. The first group of 15 mice had MCF-7 xenografts (142.3 $\pm$ 68.5 mm^3, mean $\pm$ SD) grown within the grafted human skin, and the second group of 4 mice comprised mice with graft alone (no tumor). All mice received i.v. (tail vein) injections of radiolabeled ^{131}I-BIBH-7 (total 8 μg of antibody, 13.3 μCi of radioactivity) and ^{125}I-huA33 control trace-labeled antibody (total 0.3 μg of antibody, 0.22 μCi of radioactivity) on day 22–23 p.i. of cells. Groups of skin-grafted mice with (n = 4–7) and without (n = 4–7) MCF-7 tumors were sacrificed by ethrane anesthesia at 24, 48, and 72 h p.i. and bled by cardiac puncture, with all tumors and organs resected immediately and weighed. All samples were counted in a Cobra II dual gamma scintillation counter (Packard Instruments, Canberra, Australia), which is capable of measuring the cpm of two isotopes simultaneously. Triplicate standards prepared from the injected material were counted at each time point, with tissue and tumor samples enabling calculations to be corrected for the physical decay of the isotopes. Results of the labeled antibody biodistribution over time were expressed as % ID/g. The tissue distribution data were calculated as the mean % ID/g $\pm$ SD (n = 4–7 mice) per time point. Autoradiography and liquid emulsion were used to determine the intratumoral distribution of radioactivity at 24, 48, and 72 h p.i. of radiolabeled ^{131}I-BIBH-7 as described previously (17).

Results

Morphological Analysis

SCID mice were grafted with full-thickness human foreskin, with the age of skin donors varying from 8 months to 14 years of age. After transplantation, the grafts were closely monitored for 4–6 weeks until they were fully healed. The SCID mice tolerated the transplanted skin samples with an 80% success rate. H&E-stained micrographs of skin grafts examined at various time points posttransplantation showed preservation of specific features in the epidermal and dermal layers in addition to other characteristic structures (Fig. 1*A*). From approximately day 28, the fully healed grafted human skin closely resembled nongrafted human foreskin morphologically (Fig. 1, *A* and *B*).

H&E-stained sections of MCF-7 tumors established within the dermis of grafted human foreskin were analyzed at various time points p.i. (Fig. 1*C*). Tumor nodules generally grew within the boundaries of the morphologically human skin and displayed some variation in tumor size. At all time points analyzed, all tumor xenograft samples (n = 33) were comprised of regions where the stromal content of the xenograft was very high (~50–80% of total tumor mass) and regions that were highly cellular and lacked an extensive stromal network (~20–50% of total tumor mass; Fig. 1*C*). The latter-described regions of the xenograft closely resembled MCF-7 tumors grown s.c. in control SCID mice (Fig. 1*D*) and were generally located at the lateral and inferior edges of the tumor xenograft (Fig. 1*C*). Tumors established in the presence of human skin (Fig. 1, *E* and *F*) also showed marked similarity to human breast carcinoma tissue (n = 4), as illustrated in a tumor sample obtained from a patient with infiltrating and *in situ* ductal carcinoma of the breast (Fig. 1*G*) compared with MCF-7 tumors grown in control nongrafted SCID mice (Fig. 1, *D* and *H*). The higher power H&E-stained sections clearly highlighted that MCF-7 tumor xenografts established in the human skin model had an extensive human stromal network surrounding islands of tumor cells (Fig. 1, *C, E,* and *F*). In contrast, the cells in MCF-7 xenografts established without the presence of human skin were highly cellular, with small areas of mouse stroma surrounding the parenchyma (Fig. 1, *D* and *H*). This was confirmed by double staining immunohistochemistry, where islands of Le^y-positive tumor cells surrounded by human FAP-positive fibroblastic stroma were seen in MCF-7 xenografts grown in the presence of human skin (Fig. 1*F*). In comparison, MCF-7 control xenografts had little connective tissue present and lacked FAP expression.

Growth Curves of MCF-7 Xenografts

MCF-7 breast carcinoma xenograft growth curves were established in control SCID mice and skin-grafted SCID mice. MCF-7 tumors established within the dermis of the grafted human skin displayed a significantly accelerated linear growth rate compared with MCF-7 tumors grown in the absence of the human skin graft ($P < 0.001$, t test; Fig. 2). The growth rate of xenografts in control SCID mice was slow initially and then increased more rapidly from day 13 onward (Fig. 2).

Immunohistochemical Analysis

Expression of Human HLA-A,B,C and Mouse H-2 in Grafted Skin and Tumor. Transplanted human skin samples were analyzed for human HLA-A,B,C and mouse H-2 expression. Representative sections from samples harvested at 8 weeks posttransplantation are shown in Fig. 1, *I* and *J*. Anti-HLA-A,B,C antibody reacted strongly with nucleated human cells of the dermis for up to 10 weeks after skin grafting (Fig. 1*I*). Within the dermis, there was staining of capillary endothelial cells and other cell types such as fibroblasts (Fig. 1*I*), which closely resembled HLA staining of control nongrafted human skin. Sparse staining of mouse H-2 was observed in the papillary and reticular regions of the

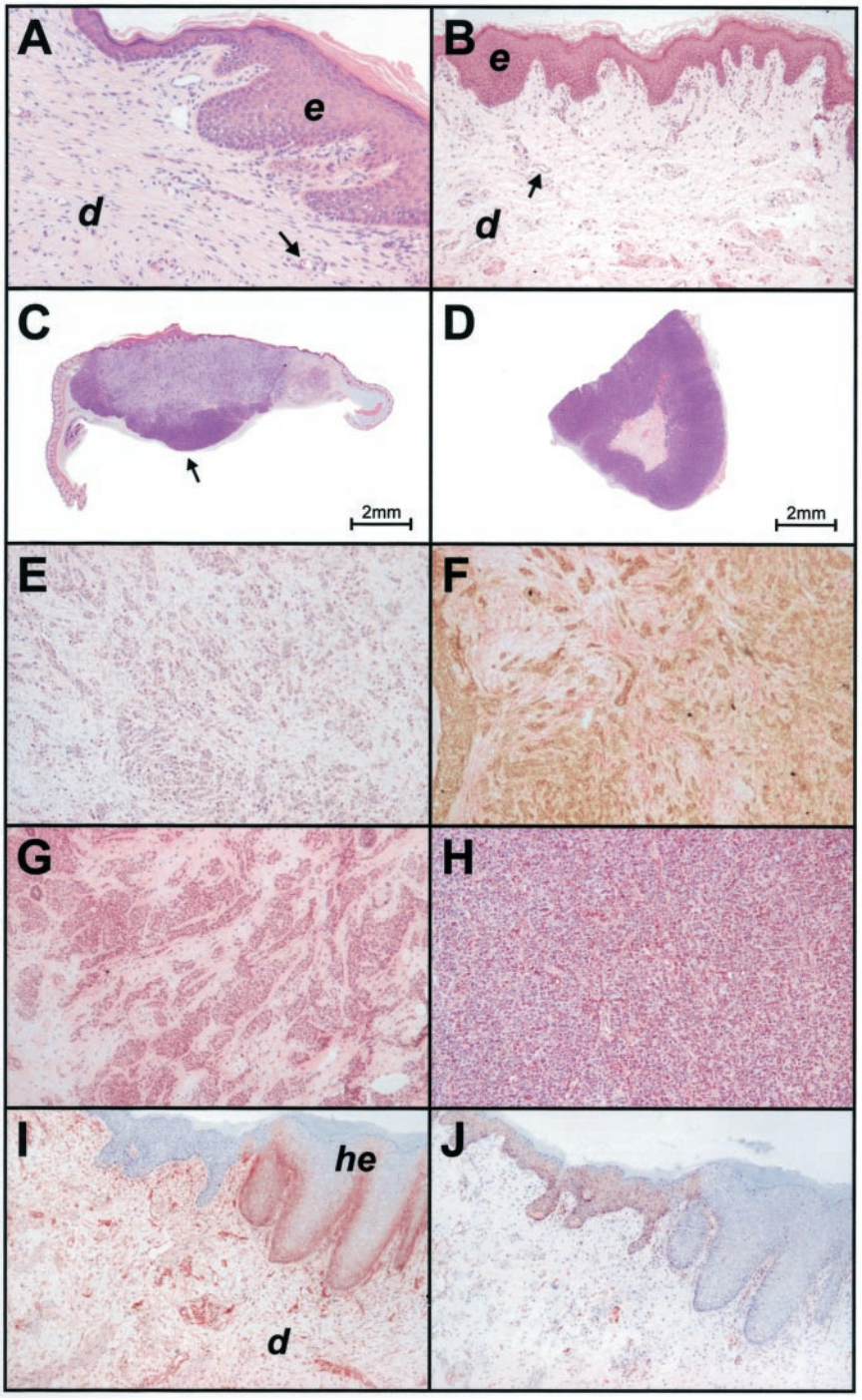

Fig. 1. A, human skin at 12 weeks posttransplantation. The skin maintains the appearance and structure of normal skin. Preservation of the epidermal (*e*) and dermal (*d*) layers, in addition to other characteristic structures such as capillary blood vessels (*arrow*), can be observed (×25). *B,* nongrafted human skin epidermal (*e*) and dermal layers (*d*), with capillary blood vessels indicated by an *arrow* (×25). *C* and *D,* mice were inoculated with 2×10^6 MCF-7 cells in grafted SCID skin and control SCID skin, respectively, and tumors were harvested at 5 weeks p.i. (*scale bar* = 2 mm). The morphological appearance of the cellular region (*arrow*) in *C* closely resembled MCF-7 tumors established s.c. in control SCID mice (*D*). *E,* MCF-7 xenograft established in the human skin graft (×10). *F,* double staining immunohistochemistry of sample *E* confirmed the presence of Le^y-positive MCF-7 cells surrounded by human FAP-positive fibroblastic stroma (×10). *G,* human breast carcinoma tissue samples (infiltrating and *in situ* ductal carcinoma) morphologically resemble MCF-7 xenografts established in the presence of the human skin (×10). *H,* xenografts established s.c. in control SCID mice (×10). Grafted human foreskin harvested at 8 weeks posttransplantation was stained for (*I*) human HLA-A,B,C and (*J*) mouse H-2 antigen expression. *I,* widespread expression of human HLA-A,B,C is seen throughout the human dermis (*d*) and hyperplasic epidermis (*he*; ×10). *J,* mouse H-2 expression throughout the dermis is sparse, but clear infiltration of H-2-positive cells is visible from the lateral edge of the epidermis (×10).

human dermis in all samples analyzed over this time period (Fig. 1*J*), with greater infiltration of murine cells into the dermis observed at 12 weeks. However, stronger expression of mouse H-2 was observed in the hypodermis or superficial fascia, which displayed minimal human HLA expression. The epidermis of the graft morphologically resembled the epidermis of normal human skin (Fig. 1*B*), with cells in the center region expressing human HLA-A,B,C, whereas cells at the lateral edges expressed mouse H-2 (Fig. 1, *I* and *J*). These changes are demonstrated by a loss in HLA-A,B,C immunoreactivity coupled with an increase in mouse H-2 expression in a morphologically appearing human epidermis (Fig. 1, *I* and *J*). This replacement of human keratinocytes and other epidermal cell subsets occurred regardless of the age of the skin donor or the size of the skin graft. In Fig. 1, *I* and *J*, some nonspecific staining of mouse sebaceous glands is observed. This was consistent in all immunohistochemical analyses performed and was observed in all control slides except

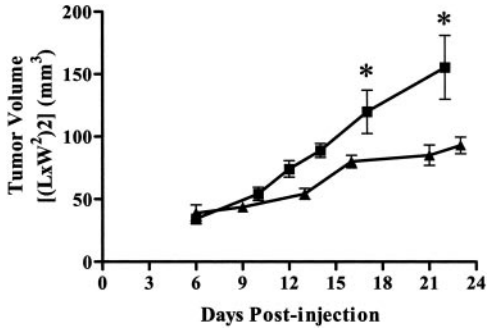

Fig. 2. Growth rate of MCF-7 tumor xenografts in human skin-grafted (■) and control non-skin-grafted (▲) SCID mice. Fifteen control SCID mice and 33 skin-grafted SCID mice were inoculated with 2×10^6 MCF-7 cells in the lateral flank on day 0, and tumor growth rate (mean tumor volume; *bars,* SD) was monitored over a 24-day period. *, $P < 0.001$ (*t* test).

for those left untreated, suggesting the possible presence of endogenous biotin in these structures. MCF-7 tumor xenografts grown within the dermis of grafted skin were also assessed for HLA-A,B,C and H-2 expression. Uniform, strong HLA-A,B,C staining was observed in these tumor sections, with smaller pockets of human HLA expression observed at the periphery of the tumor. In contrast, the peripheral regions expressed mouse H-2, which stained the tumor connective tissue surrounding islands of cells (data not shown).

Analysis of Human FAP Expression in Human Skin Grafts. To evaluate the expression of human FAP within human skin grafts, harvested samples were immunostained with the mF19 antibody. This antibody is specific for human FAP and does not cross-react with the murine FAP counterpart. Widespread expression of human FAP was observed throughout the majority of the human graft dermis, particularly the papillary region, over the 12-week period of study (representative staining is shown in Fig. 3, *A* and *B*). Human FAP expression colocalized with human HLA-A,B,C staining, further demonstrating the human derivation of the fibroblastic cells. The hypodermis (which is comprised mostly of mouse adipose tissue) and mouse skin predominantly lacked FAP-positive reactive fibroblasts. At 2–3 weeks posttransplantation, nonspecific staining was observed in the reforming epidermal layer (Fig. 3*A*). This observation was consistent in all tissue samples harvested at this time point posttransplantation and was not apparent at later time points.

Analysis of Human FAP Expression in MCF-7 Xenografts. MCF-7 breast carcinoma xenografts were also analyzed for FAP expression. Reactive stromal fibroblasts (comprising ~50–80% of the total tumor mass) were observed in all MCF-7 tumors established within a human skin graft over the 9-week period of study (representative staining is shown in Fig. 3, *C* and *D*) at 3 weeks p.i., again colocalizing with regions of HLA-A,B,C immunoreactivity. Stroma was a minor component of the tumor in highly cellular regions (Fig. 3*C*). In control MCF-7 xenografts grown in SCID mice without the presence of human skin, no staining was observed (data not shown), indicating the absence of human FAP-positive stroma. MCF-7 tumors were confirmed positive for Le^y expression at all time points using the m3S193 mAb (data not shown).

Expression of Human Vascular Antigens. Human skin grafts and adjacent control SCID skin and MCF-7 xenografts grown in the presence of human skin were harvested at sequential time points posttransplantation and evaluated with antibodies against human endoGlyx-1, human PECAM-1, and mouse PECAM-1. PECAM-1 and endoGlyx-1 were selected because their baseline level of antigen expression is high in all blood vessels (19, 20). Human blood vessel antigens were seen throughout the entire human skin graft, for up to 12 weeks posttransplantation, correlating with regions where human HLA-A,B,C and human FAP expression had been demonstrated (Fig. 3, *E* and *F*). These blood vessels were randomly organized, with smaller capillary vessels having a more flattened appearance (Fig. 3*F*). Similar levels of vessel density were observed with both the PECAM-1 and endoGlyx-1 antibodies, which stained identical vessels. Murine blood vessels were detected by 2 weeks posttransplantation, primarily at the lateral and inferior edges of the graft, but they became more prominent from 3 weeks and beyond, where they coexisted at similar or lower levels with blood vessels expressing human antigens, for up to 10 weeks posttransplantation. At 12 weeks after grafting, mouse vessels became more prevalent in the samples analyzed. The staining pattern of human PECAM-1 and endoGlyx-1 in MCF-7 xenografts grown within the grafted human skin was comparable, and expression of these antigens on human vessels was most prominent in the median zone of the xenograft (close to the graft epidermis; representative staining is shown in Fig. 3*G*), in areas that were also shown to be positive for human FAP and HLA-A,B,C. This staining pattern was observed in the majority of tumor samples analyzed, independent of time point. Mouse blood vessels were also detectable throughout tumor nodules (Fig. 3*H*); they coexisted with the human vascular supply at similar or greater levels.

In Vivo Targeting of Human Stromal FAP in MCF-7 Breast Carcinoma Xenografts

The radiochemical purity of all radiolabeled constructs was confirmed to be ≥98.5% using instant thin layer chromatography. A Lindmo assay was performed for ^{131}I-BIBH-7 to evaluate the antigen-binding capacity of the antibody after radiolabeling. The binding curve reached saturation, displaying high antigen binding and immunoreactivity (>95%). Scatchard affinity analysis was used to calculate the apparent association constant of ^{131}I-BIBH-7 (9.73×10^8), and radiolabeled constructs were also assessed for serum stability properties by single-point immunoreactivity assay. ^{131}I-BIBH-7 displayed ~15% loss in binding capacity between day 0 (99.3%) and day 1 (84.4%), followed by an additional ~15% loss by day 5 (68.6%). No further loss in immunoreactivity was observed between day 5 and day 7 (67.2%). The *in vivo* targeting potential of the iodinated antibody was assessed in SCID mice grafted with human skin, bearing MCF-7 tumor xenografts that express the human FAP antigen on stromal fibroblasts. The tumor, blood, and normal tissue retention was determined at 24, 48, and 72 h p.i. Nonspecific uptake was concurrently evaluated using the ^{125}I-huA33 isotype-matched control antibody. After injection, maximal MCF-7 tumor uptake was observed at 72 h p.i. (12.47 ± 2.8% ID/g, mean ± SD; Fig. 4*A*),

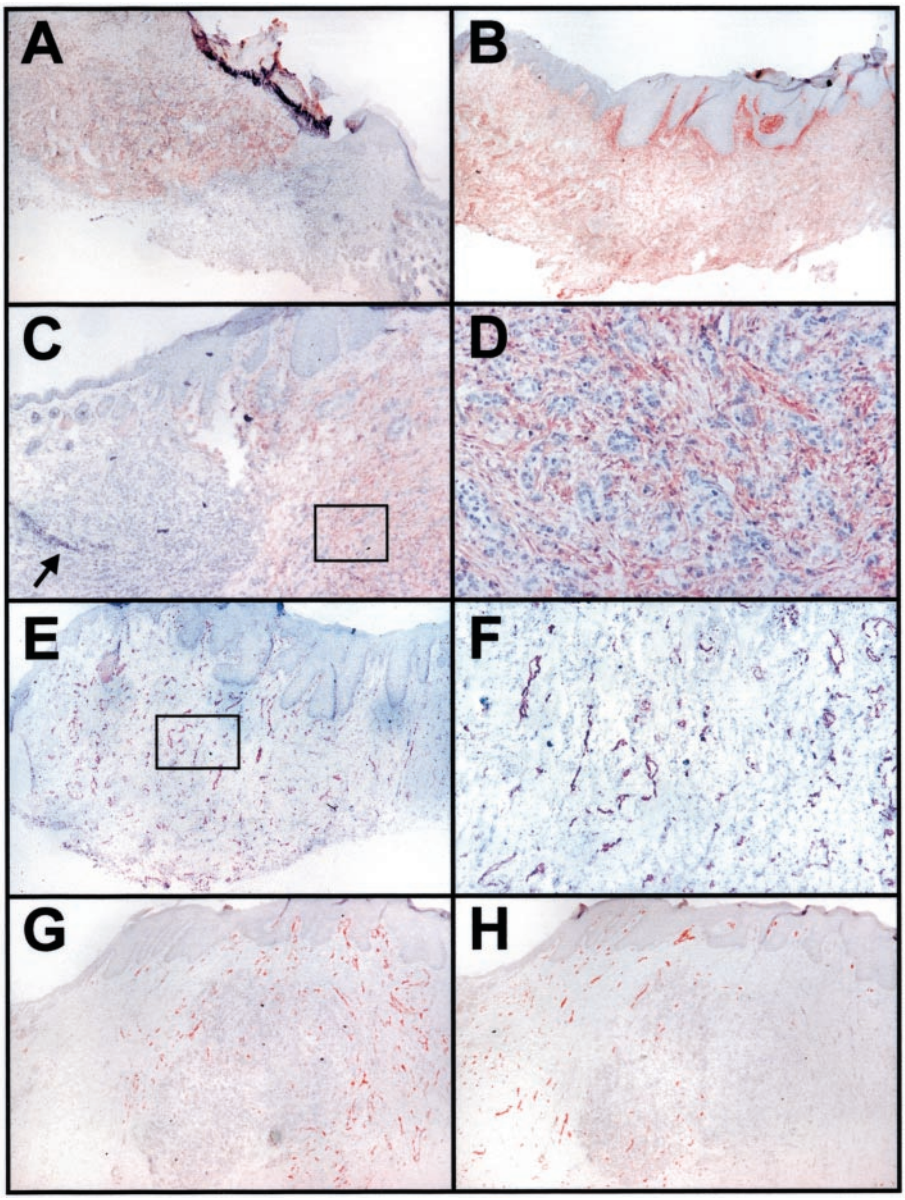

Fig. 3. *A* and *B,* FAP expression in grafted human skin harvested at 2 and 8 weeks posttransplantation, respectively. Tumors were resected and stained with an antihuman FAP mAb. *C,* expression of human FAP in MCF-7 xenografts grown within the transplanted human skin at 3 weeks p.i. Staining is less prominent in the more cellular region (*arrow*) of the tumor, where the stromal content is reduced (×4). *D,* at a higher power magnification of the *boxed region* in *C*, specific staining of the tumor stromal compartment was observed, with no staining of tumor cells that do not express FAP (×10). *E,* expression of human PECAM-1 in grafted human skin at 8 weeks posttransplantation (×4); *F,* a higher power magnification of the *boxed region* in *E* (×10). Expression of (*G*) human and (*H*) mouse PECAM-1 in MCF-7 xenografts grown within the transplanted human skin and resected at 4 weeks p.i. (×4).

with a tumor:blood ratio of 2.3:1. At this time point, nonspecific accumulation of the control ^{125}I-huA33 antibody to the tumor reached a mean ± SD of 5.56 ± 2.6% ID/g. The ^{131}I-BIBH-7 and ^{125}I-huA33 control antibody also displayed high uptake in skin graft alone (Fig. 4*A*). No unexpected localization was observed in other normal tissues investigated. The intratumoral distribution of ^{131}I-BIBH-7 was determined by direct autoradiography and emulsion film, and both analyses illustrated specific localization of radioactivity to the tumor stromal compartment (Fig. 4*B*). Immunohistochemistry confirmed the presence of human FAP-positive fibroblasts and Le^{y}-positive neoplastic cells in the tumor xenografts (Fig. 1*F*).

Discussion

The targeting of antigens selectively expressed on the surface of tumor stromal fibroblasts or tumor capillary endothelial cells is currently being explored for the immunotherapy of cancer (9, 10, 21). By targeting or preventing the generation of tumor stroma or angiogenic blood vessels, tumor lesions may be deprived of the essential support services or nutrients required for survival and growth (1). The main challenge for this approach is to identify target molecules with suitably restricted expression patterns in normal tissues.

The abundant and consistent expression of the FAP protein on fibroblastic cells within epithelial tumor stroma, combined with the absence of FAP expression on normal resting fibrocytes, makes it one of the most important antigens for targeted therapy of tumor stroma. The close proximity of fibroblasts to the tumor vasculature suggests that they would be highly accessible to circulating mAbs (22). Furthermore, unlike the malignant epithelial cells of carcinomas, activated fibroblasts are not genetically transformed, and they also do

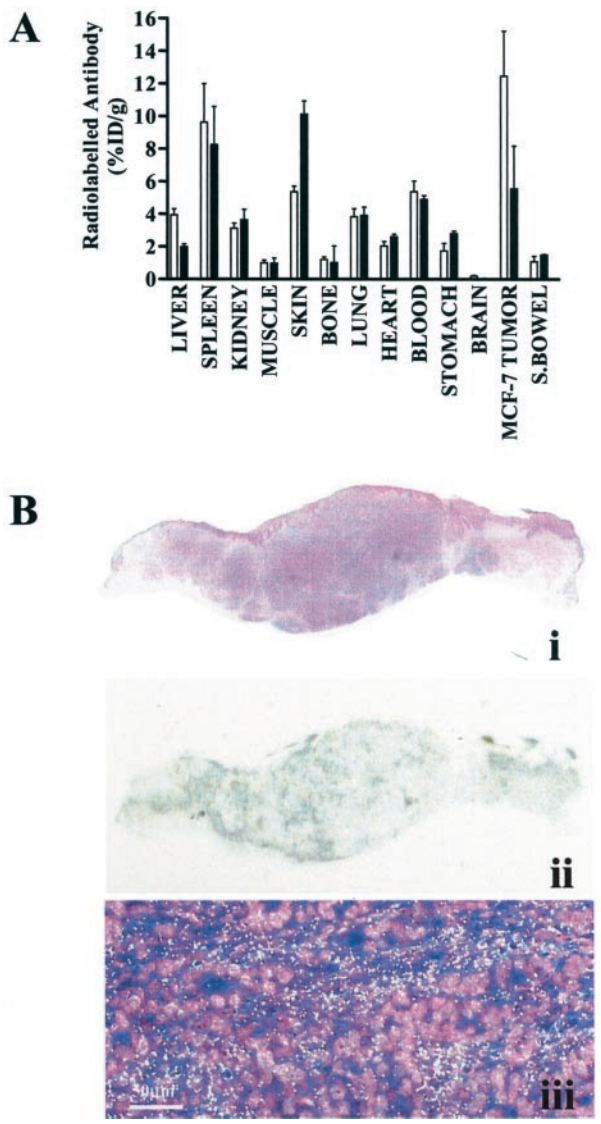

Fig. 4. A, tissue distribution at 72 h p.i. of ^{131}I-BIBH-7 (□) and control ^{125}I-huA33 (■) mAbs in skin-grafted SCID mice bearing MCF-7 tumors. *B, i,* H&E-stained section shows the morphology and architecture of the tumor nodule. *B, ii,* localization of ^{131}I-BIBH-7 radioconjugate to the tumor is visualized by autoradiography. *B, iii,* the *white grains* in the dark-field emulsion image indicate specific localization of ^{131}I-BIBH-7 to the stromal compartment, with minimal uptake in the parenchyma (*scale bar* = 50 μm).

not display the genetic and phenotypic heterogeneity observed in malignant cells (23–26), hence the outgrowth of antigen-loss variants or mutants is less likely to occur. The preclinical evaluation of antihuman FAP mAbs has been impeded by the absence of a relevant tumor animal model that can confirm that anti-FAP antibodies may selectively accumulate in human tumor tissues. This study reports on the first characterized animal xenograft model of human FAP expression. Similar models have been established previously by other groups to study a variety of disease pathologies (13–15, 27–29). Results from these studies indicate that human skin/SCID mouse chimera models can provide a microenvironment in which neoplasia and issues concerning normal human skin biology can be explored. We have used this model to explore and characterize, for the first time, the expression of human stromal antigens in xenografts and demonstrate the ability to target the stromal antigen FAP *in vivo*.

Human skin grafted on to the lateral flank of SCID mice was well tolerated, phenotypically resembled normal human skin by 4–5 weeks posttransplantation, and preserved its morphology for up to 3 months (Fig. 1, *A* and *B*). These observations correlate with the findings of Yan *et al.* (13) and others (27, 30, 31). It was also observed that the epidermis was often hyperplasic and hyperkeritanized with irregular proliferation of the rete ridges and corresponding elongated papillae (Fig. 1*A*). This could be a reaction to chronic irritation such as scratching by the mice while grooming the graft (32). Tumor xenografts established within the dermis of grafted human skin resembled morphologically infiltrating *in situ* ductal carcinoma of the breast (Fig. 1, *E–G*). At the inferior graft margin, areas of high cell density were observed in MCF-7 xenografts established within the transplanted graft dermis; this was presumably because of the proximity of this region to mouse tissue and the absence of fibroblasts in skin hypodermis (Fig. 1*C*; Ref. 33). Growth curves established in control SCID and skin-grafted SCID mice, indicated a significantly accelerated growth rate in skin-grafted SCID mice (Fig. 2). This apparent growth advantage may have been imparted by the human stromal and vessel elements present in the skin-grafted mice, which may have promoted xenograft growth in the early stages after inoculation of cells.

Grafted human skin and xenografts established within the dermis of grafted skin were harvested at sequential time points posttransplantation and characterized extensively for the expression of human antigenic markers to assess whether there were modulations in antigen expression and to determine how long the skin would maintain its human phenotype. Widespread and uniform expression of human HLA-A,B,C was observed for up to 3 months after grafting in the papillary and reticular regions of the human dermis. However, HLA-A,B,C-positive cells were minimally expressed in the hypodermis or superficial fascia, compared with positive staining in control skin, which is most likely attributable to the close proximity of this layer with mouse tissue. Expression of mouse H-2 by phenotypically human epidermal cells was observed to occur with time at the periphery of the skin graft. These regions overlayed a characteristically human dermis (Fig. 1*J*) and were most likely due to a re-epithelialization process by mouse cells at marginal sites (31). These results indicated the dynamic interaction of the mouse and human microenvironment in this system and were not surprising, considering that epidermal cells are renewed approximately every 15–30 days (33). Reports by other investigators have demonstrated the presence of a predominantly human epidermis in full-thickness human skin transplants (13, 27).

Activated human fibroblasts were uniformly distributed in the transplanted skin dermis for up to 3 months after skin grafting, demonstrating that the human skin graft behaves as a normal healing wound (Refs. 1, 20, and 34; Fig. 3, *A* and *B*). In agreement with these findings was a report by Demarchez *et al.* (35), which demonstrated the presence of human stromal factors including type I collagen, elastic fibers, and mes-

enchymal cells in the dermis of split-thickness skin grafted on to *nude* mice. Human breast carcinoma MCF-7 xenografts grown in the dermis of the grafted human skin were also examined for the presence of FAP-positive fibroblasts (Fig. 3, *C* and *D*), which were found in human skin/SCID but not control xenografts for up to 9 weeks p.i. Colocalization of human FAP with human HLA-A,B,C was observed in all samples analyzed, further demonstrating the human derivation of the FAP-positive fibroblasts. These results illustrate that the graft is undergoing wound healing and that the presence of human skin also encourages the formation of a tumor stroma that is comprised predominantly of human FAP-expressing fibroblasts. The formation of the tumor stromal compartment very closely resembles the process observed with granulation tissue in wound healing, with both processes also accompanied by neovascularization (36–38).

In this model, human blood vessels were characterized by antihuman PECAM-1 and endoGlyx-1 antibodies. In transplanted human skin, human vessels were prominent for up to 10 weeks posttransplantation, with a slight decrease in vessel density observed at 12 weeks after grafting (Fig. 3, *E* and *F*). These results are consistent with published studies investigating human vessel expression patterns in full-thickness human skin grafts on SCID mice (13–15, 27, 39, 40), which reported the coexistence of human and mouse vessels or the complete absence of a mouse vascular supply from the grafted human skin. It is possible that the graft becomes vascularized by anastamoses of human graft vessels to recipient host vessels (41, 42), or alternatively, revascularization may occur by the direct ingrowth of host vessels (43). This emphasizes the importance of ensuring proper apposition of the graft with the recipient bed during the grafting procedure (41, 44, 45) and avoiding excessive disturbance of the aligned wound margin (42, 45, 46), which is difficult to achieve with rodents. In xenografts established in the grafted human skin, human vessels were prevalent in regions positive for human FAP and HLA-A,B,C expression (Fig. 3, *G* and *H*). Observations by other investigators (15, 27) suggested that tumor xenografts (breast and melanoma, respectively) established in human skin grafts are predominantly supported by a human vasculature. The revascularization of grafted and nongrafted human neoplastic tissue has not been extensively explored; however, in studies where tumor tissue was grafted to the chick chorioallantoic membrane, the tumor grafts acquired their blood supply solely from the host microvasculature (47).

The immunohistochemistry results indicated that the established tumor xenograft model provides an ideal microenvironment for targeting FAP-expressing fibroblasts of the stroma. Hence, a biodistribution analysis was undertaken with a ^{131}I-labeled mAb that specifically targets the FAP antigen. The newly validated system is the first description of stromal targeting with an anti-FAP mAb. The ^{131}I-BIBH-7 radioconjugate displayed excellent radiochemical purity, immunoreactivity, and affinity data. The serum stability study indicated a gradual loss in immunoreactivity for ^{131}I-BIBH-7. This slight loss in immunoreactivity is often observed with intact antibody constructs over 7 days of incubation in human serum at 37°C. Maximal tumor uptake was observed at 72 h p.i., reaching 12.47 $\pm$ 2.76% ID/g (Fig. 4*A*). This specific uptake in the tumor xenograft, which was also visualized with autoradiography and emulsion film (Fig. 4*B*), is favorable, considering that the FAP-positive stroma contributed between 50% and 80% of the tumor mass. Uptake in the skin graft alone was most probably due to (*a*) the hyperpermeable human vessels present in the skin graft resulting in increased uptake in skin graft alone, as supported by graft uptake observed with the ^{125}I-huA33 isotype matched control, and (*b*) the presence of human FAP in the human skin graft. At all time points, uptake in the target MCF-7 human FAP-expressing tumor xenograft was higher than that of the control ^{125}I-huA33 antibody, which was administered simultaneously, indicating limited nonspecific binding in tumor. The normal tissue distribution was very similar for both radioconjugates, with only slightly high uptake observed in the spleen. High splenic uptake was observed in all biodistribution studies performed using this animal model system and is most likely due to binding of the radioconjugate to splenic Fc receptors.

The results described in this paper report the first characterized animal model of human FAP expression both in wound healing and in a human carcinoma xenograft. The developed and characterized human skin/SCID model is a powerful tool that has potential relevance to a range of scientific and therapeutic investigations. The effects of stromal ablation on tumor cell growth and antigen expression can be defined in this model, and we are presently undertaking such studies. Antibody mixtures targeting different tumor compartments simultaneously, such as tumor cell surface and stroma, may also be evaluated in this model, with the aim of developing improved cancer therapies (11, 30, 48, 49). The validated model is also very suited for investigations that link anti-FAP antibodies, lower molecular weight anti-FAP constructs, anti-FAP inhibitors, and antiangiogenic molecules with novel isotopes such as Bismuth-212 and Astatine-211. The relationship between the stroma of tumors and tumor cells, including autocrine and paracrine signaling pathways, as well as integrin/matrix interactions may also be explored.

References

1. Dvorak, H. F. Tumors: wounds that do not heal. Similarities between tumor stroma generation and wound healing. N. Engl. J. Med., *315:* 1650–1659, 1986.

2. Garin-Chesa, P., Old, L. J., and Rettig, W. J. Cell surface glycoprotein of reactive stromal fibroblasts as a potential antibody target in human epithelial cancers. Proc. Natl. Acad. Sci. USA, *87:* 7235–7239, 1990.

3. Niedermeyer, J., Enenkel, B., Park, J. E., Lenter, M., Rettig, W. J., Damm, K., and Schnapp, A. Mouse fibroblast-activation protein-conserved Fap gene organization and biochemical function as a serine protease. Eur. J. Biochem., *254:* 650–654, 1998.

4. Scanlan, M. J., Raj, B. K., Calvo, B., Garin-Chesa, P., Sanz-Moncasi, M. P., Healey, J. H., Old, L. J., and Rettig, W. J. Molecular cloning of fibroblast activation protein α, a member of the serine protease family selectively expressed in stromal fibroblasts of epithelial cancers. Proc. Natl. Acad. Sci. USA, *91:* 5657–5661, 1994.

5. Park, J. E., Lenter, M. C., Zimmermann, R. N., Garin-Chesa, P., Old, L. J., and Rettig, W. J. Fibroblast activation protein, a dual specificity serine protease expressed in reactive human tumor stromal fibroblasts. J. Biol. Chem., *274:* 36505–36512, 1999.

6. Rettig, W. J., Garin-Chesa, P., Beresford, H. R., Oettgen, H. F., Melamed, M. R., and Old, L. J. Cell-surface glycoproteins of human sarco-

mas: differential expression in normal and malignant tissues and cultured cells. Proc. Natl. Acad. Sci. USA, *85:* 3110–3114, 1988.

7. Abbott, C. A., Yu, D. M., Woollatt, E., Sutherland, G. R., McCaughan, G. W., and Gorrell, M. D. Cloning, expression and chromosomal localization of a novel human dipeptidyl peptidase (DPP) IV homolog, DPP8. Eur. J. Biochem., *267:* 6140–6150, 2000.

8. Ariga, N., Sato, E., Ohuchi, N., Nagura, H., and Ohtani, H. Stromal expression of fibroblast activation protein/seprase, a cell membrane serine proteinase and gelatinase, is associated with longer survival in patients with invasive ductal carcinoma of breast. Int. J. Cancer, *95:* 67–72, 2001.

9. Burrows, F. J., and Thorpe, P. E. Vascular targeting: a new approach to the therapy of solid tumors. Pharmacol. Ther., *64:* 155–174, 1994.

10. Old, L. J. Immunotherapy for cancer. Sci. Am., *275:* 136–143, 1996.

11. Scott, A. M., and Cebon, J. Clinical promise of tumour immunology. Lancet, *349* (Suppl. 2)*:* SII19–SII22, 1997.

12. Soule, H. D., Vazguez, J., Long, A., Albert, S., and Brennan, M. A human cell line from a pleural effusion derived from a breast carcinoma. J. Natl. Cancer Inst. (Bethesda), *51:* 1409–1416, 1973.

13. Yan, H. C., Juhasz, I., Pilewski, J., Murphy, G. F., Herlyn, M., and Albelda, S. M. Human/severe combined immunodeficient mouse chimeras. An experimental *in vivo* model system to study the regulation of human endothelial cell-leukocyte adhesion molecules. J. Clin. Investig., *91:* 986–996, 1993.

14. Soballe, P. W., Montone, K. T., Satyamoorthy, K., Nesbit, M., and Herlyn, M. Carcinogenesis in human skin grafted to SCID mice. Cancer Res., *56:* 757–764, 1996.

15. Brooks, P. C., Stromblad, S., Klemke, R., Visscher, D., Sarkar, F. H., and Cheresh, D. A. Antiintegrin $\alpha_v\beta_3$ blocks human breast cancer growth and angiogenesis in human skin. J. Clin. Investig., *96:* 1815–1822, 1995.

16. Nonoyama, S., Smith, F. O., Bernstein, I. D., and Ochs, H. D. Strain-dependent leakiness of mice with severe combined immune deficiency. J. Immunol., *150:* 3817–3824, 1993.

17. Clarke, K., Lee, F. T., Brechbiel, M. W., Smyth, F. E., Old, L. J., and Scott, A. M. *In vivo* biodistribution of a humanized anti-Lewis Y monoclonal antibody (hu3S193) in MCF-7 xenografted BALB/c nude mice. Cancer Res., *60:* 4804–4811, 2000.

18. Lee, F. T., Hall, C., Rigopoulos, A., Zweit, J., Pathmaraj, K., O'Keefe, G. J., Smyth, F. E., Welt, S., Old, L. J., and Scott, A. M. Immuno-PET of human colon xenograft-bearing BALB/c nude mice using ^{124}I-CDR-grafted humanized A33 monoclonal antibody. J. Nucl. Med., *42:* 764–769, 2001.

19. Albelda, S. M., and Buck, C. A. Integrins and other cell adhesion molecules. FASEB J., *4:* 2868–2880, 1990.

20. Damjanovich, L., Albelda, S. M., Mette, S. A., and Buck, C. A. Distribution of integrin cell adhesion receptors in normal and malignant lung tissue. Am. J. Respir. Cell Mol. Biol., *6:* 197–206, 1992.

21. Dvorak, H. F., Nagy, J. A., and Dvorak, A. M. Structure of solid tumors and their vasculature: implications for therapy with monoclonal antibodies. Cancer Cells, *3:* 77–85, 1991.

22. Rettig, W. J., Garin-Chesa, P., Healey, J. H., Su, S. L., Ozer, H. L., Schwab, M., Albino, A. P., and Old, L. J. Regulation and heteromeric structure of the fibroblast activation protein in normal and transformed cells of mesenchymal and neuroectodermal origin. Cancer Res., *53:* 3327–3335, 1993.

23. Cullen, K. J., Smith, H. S., Hill, S., Rosen, N., and Lippman, M. E. Growth factor messenger RNA expression by human breast fibroblasts from benign and malignant lesions. Cancer Res., *51:* 4978–4985, 1991.

24. Basset, P., Bellocq, J. P., Wolf, C., Stoll, I., Hutin, P., Limacher, J. M., Podhajcer, O. L., Chenard, M. P., Rio, M. C., and Chambon, P. A novel metalloproteinase gene specifically expressed in stromal cells of breast carcinomas. Nature (Lond.), *348:* 699–704, 1990.

25. Pyke, C., Ralfkiaer, E., Tryggvason, K., and Dano, K. Messenger RNA for two type IV collagenases is located in stromal cells in human colon cancer. Am. J. Pathol., *142:* 359–365, 1993.

26. Rettig, W. J., Su, S. L., Fortunato, S. R., Scanlan, M. J., Raj, B. K., Garin-Chesa, P., Healey, J. H., and Old, L. J. Fibroblast activation protein: purification, epitope mapping and induction by growth factors. Int. J. Cancer, *58:* 385–392, 1994.

27. Juhasz, I., Albelda, S. M., Elder, D. E., Murphy, G. F., Adachi, K., Herlyn, D., Valyi-Nagy, I. T., and Herlyn, M. Growth and invasion of human melanomas in human skin grafted to immunodeficient mice. Am. J. Pathol., *143:* 528–537, 1993.

28. Nickoloff, B. J., Kunkel, S. L., Burdick, M., and Strieter, R. M. Severe combined immunodeficiency mouse and human psoriatic skin chimeras. Validation of a new animal model. Am. J. Pathol., *146:* 580–588, 1995.

29. Juhasz, I., Simon, M., Jr., Herlyn, M., and Hunyadi, J. Repopulation of Langerhans cells during wound healing in an experimental human skin/SCID mouse model. Immunol. Lett., *52:* 125–128, 1996.

30. McKearn, T. J. Radioimmunodetection of solid tumors. Future horizons and applications for radioimmunotherapy. Cancer (Phila.), *71:* 4302–4313, 1993.

31. Kaufmann, R., Mielke, V., Reimann, J., Klein, C. E., and Sterry, W. Cellular and molecular composition of human skin in long-term xenografts on SCID mice. Exp. Dermatol., *2:* 209–216, 1993.

32. Curren, R. C. Colour Atlas of Histopathology. London: Bailliere, Tindall and Cassell, 1969.

33. Junqueira, L. C., Carneiro, J., and Kelley, R. O. Basic Histology, 8th ed. London: Prentice Hall International, 1995.

34. van den Hooff, A. Stromal involvement in malignant growth. Adv. Cancer Res., *50:* 159–196, 1988.

35. Demarchez, M., Hartmann, D. J., Herbage, D., Ville, G., and Prunieras, M. Wound healing of human skin transplanted onto the nude mouse. II. An immunohistological and ultrastructural study of the epidermal basement membrane zone reconstruction and connective tissue reorganization. Dev. Biol., *121:* 119–129, 1987.

36. Gerwins, P., Skoldenberg, E., and Claesson-Welsh, L. Function of fibroblast growth factors and vascular endothelial growth factors and their receptors in angiogenesis. Crit. Rev. Oncol. Hematol., *34:* 185–194, 2000.

37. Norrby, K. Angiogenesis: new aspects relating to its initiation and control. APMIS, *105:* 417–437, 1997.

38. Sieweke, M. H., and Bissell, M. J. The tumor-promoting effect of wounding: a possible role for TGF-β-induced stromal alterations. Crit. Rev. Oncog., *5:* 297–311, 1994.

39. Baluna, R., and Vitetta, E. S. An *in vivo* model to study immunotoxin-induced vascular leak in human tissue. J. Immunother., *22:* 41–47, 1999.

40. Christofidou-Solomidou, M., Bridges, M., Murphy, G. F., Albelda, S. M., and DeLisser, H. M. Expression and function of endothelial cell α_v integrin receptors in wound-induced human angiogenesis in human skin/SCID mice chimeras. Am. J. Pathol., *151:* 975–983, 1997.

41. Ratner, D., Viron, A., Puvion-Dutilleul, F., and Puvion, E. Pilot ultrastructural evaluation of human preauricular skin before and after high-energy pulsed carbon dioxide laser treatment. Arch. Dermatol., *134:* 582–587, 1998.

42. Aston, S. J., Beasley, R. W., and Thorne, C. H. M. Grabb and Smith's Plastic Surgery, 5th ed. Philadelphia: Lippincott-Raven Publishers, 1997.

43. Chick, L. R. Brief history and biology of skin grafting. Ann. Plast. Surg., *21:* 358–365, 1988.

44. Black, J. M. Surgical options in wound healing. Crit. Care Nurs. Clin. North Am., *8:* 169–182, 1996.

45. Kinner, M. A., and Daly, W. L. Skin transplantation. Crit. Care Nurs. Clin. North Am., *4:* 173–178, 1992.

46. Silkiss, R. Z., Glasgow, B. J., and Baylis, H. I. Revascularization studies of an opposing eyelid pedicle flap. Ophthal. Plast. Reconstr. Surg., *5:* 110–117, 1989.

47. Ausprunk, D. H., Knighton, D. R., and Folkman, J. Vascularization of normal and neoplastic tissues grafted to the chick chorioallantois. Role of host and preexisting graft blood vessels. Am. J. Pathol., *79:* 597–628, 1975.

48. Mukerjee, S., McKnight, M. E., Nasoff, M., and Glassy, M. C. Co-expression of tumor antigens and their modulation by pleiotrophic modifiers enhance targeting of human monoclonal antibodies to pancreatic carcinoma. Hum. Antibodies, *9:* 9–22, 1999.

49. Rowland, A. J., McKenzie, I. F., and Pietersz, G. A. Enhanced antitumour effects using a combination of two antibodies conjugated to different drugs. J. Drug Target., *2:* 113–121, 1994.